Interference Analysis and Resource Allocation for TDD-CDMA Systems to Support Asymmetric Services by Using Directional Antennas

Li-Chun Wang, *Member, IEEE*, Shi-Yen Huang, and Yu-Chee Tseng

***Abstract*—This paper explores the advantages of using directional antennas in time division duplex (TDD) code division multiple access (CDMA) systems to support asymmetric traffic services. In the TDD-CDMA system, the transmission for asymmetric traffic from neighboring cells may cause the cross-slot interference, which can seriously degrade system capacity. To avoid the cross-slot interference for TDD-CDMA systems, many current resource allocation algorithms typically require a global control on the transmission direction (either downlink or uplink) in each time slot. Apparently, this requirement substantially constrains the flexibility of TDD-CDMA systems to deliver asymmetric traffic services in a more practical situation where every cell may have different uplink and downlink bandwidth requirements. We analyze the interference of the TDD-CDMA system with a trisector cellular architecture, where three directional antennas are employed at each base station. We find that the directivity of directional antennas can provide an additional degree of freedom for allocating radio resource. Taking advantage of this property, we introduce the concept of *virtual cell*, defined as the same converge area of a cell but is composed of three sectors from the three adjacent base stations. Furthermore, we propose a new virtual cell-based distributed code/time slot allocation algorithm to enable a TDD-CDMA system to provide asymmetric services with *different* rates of asymmetry in *every* cell coverage area. We demonstrate that the proposed algorithm does not only offer more flexibility in handling nonuniform traffic patterns, but maintain good radio link performance and call blocking performance.**

***Index Terms*—Code division multiple access (CDMA), opposition direction interference, resource allocation, time duplex division (TDD).**

I. Introduction

CODE DIVISION MULTIPLE ACCESS (CDMA) systems comprise of two operation modes, namely frequency division duplex (FDD) and time division duplex (TDD). In FDD-CDMA systems, a pair of frequency bands are used for uplink and downlink transmissions. In TDD-CDMA systems, the uplink and downlink transmissions are multiplexed into time slots on the same frequency band. The key advantage of the TDD-CDMA system is its capability of flexibly adjusting uplink and downlink bandwidth by allocating different numbers of time slots [1]. Thus, compared to the FDD-CDMA system, the TDD-CDMA system is more suitable for applications with asymmetric traffic, such as Internet browsing, file transfer, etc.

Manuscript received July 4, 2003; revised May 12, 2004 and October 4, 2004. Some results in this paper were presented at the IEEE VTC'02 Spring, May 2002. This work was supported in part by the Lee and MTI Center for Networking Research, and the National Science Council R.O.C. under Contract 90-2213-E-009-068, 89-E-FA06-2-4, and EX-91-E-FA06-4-4. The work of Y. C. Tseng was supported in part by the NSC Program for Promoting Academic Excellence of Universities by Grant 93-2752-E-007-001-PAE, by the Computer and Communications Research Labs, ITRI, Taiwan, by Intel Inc., by the Institute for Information Industry, and MOEA, R.O.C., under the Handheld Device Embedded System Software Technology Development Project and the Communications Software Technology Project, and by the Chung-Shan Institute of Science and Technology under Contract BC93B12P. The review of this paper was coordinated by Prof. S.-L. Kim.

L.-C. Wang and S.-Y. Huang are with the Department of Communication Engineering, National Chiao Tung University, Hsinchu, Taiwan (e-mail: lichun@cc.nctu.edu.tw).

Y.-C. Tseng is with the Department of Computer Science and Information Engineering, National Chiao Tung University, Hsinchu, Taiwan.

Digital Object Identifier 10.1109/TVT.2005.844660

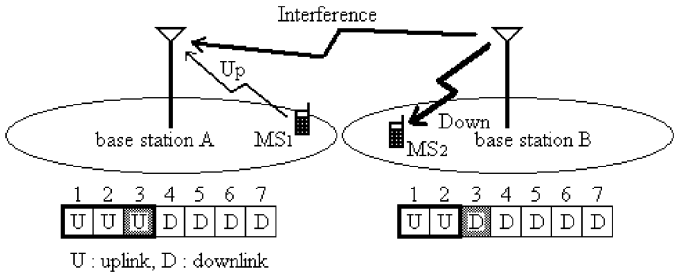

Fig. 1. An example of cross-slot interference. In this example, during slot 3, base station B causes the cross-slot interference to MS1's transmission.

However, the transmission of asymmetric traffic from adjacent cells in the TDD-CDMA system may cause the *cross-slot interference*, which will seriously degrade system capacity. In TDD-CDMA systems, we usually define the switching point as the boundary between uplink time slots and downlink time slots within a transmission frame. If two neighboring cells have different switching points due to distinct uplink-to-downlink traffic ratios, then there may exist some time slots that are used for downlink transmissions in one cell, but for uplink transmissions in the other cell. In this paper, we call the interference due to the opposite-direction transmissions between two neighboring cells the *cross-slot interference*. Fig. 1 illustrates a typical example of the cross-slot interference in the TDD-CDMA system. In this example, time slot 3 is used for the uplink transmission by base station A, while also being used for the downlink transmission by base station B. Note that the transmission power of a base station is much higher than that of a mobile terminal. This may interfere the reception quality of base station A. As a consequence, it is usually suggested that the *same* time slot be used for the *same* transmission direction for two neighboring cells, unless one of them is willing to leave the slot unused. Apparently, this approach may waste slot resources because neighboring cells do not necessarily have the same traffic patterns. Consequently, this requirement significantly limits the key advantages of the TDD system to support asymmetric traffic services.

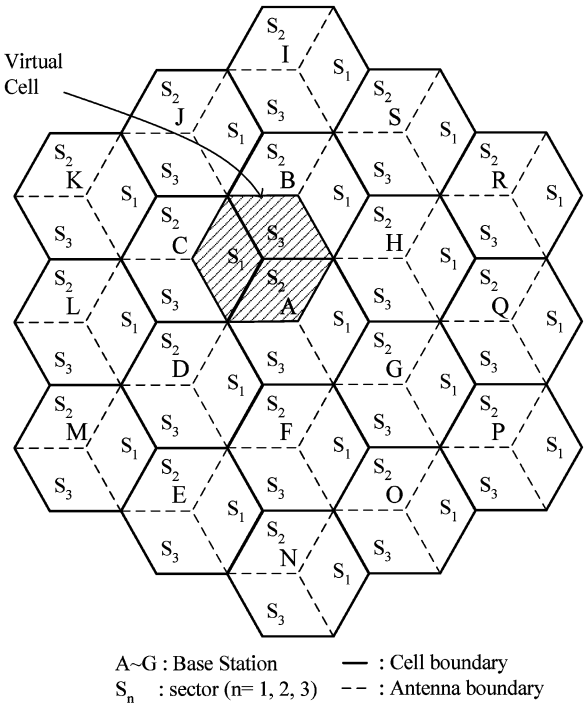

Fig. 2. A trisector cellular system.

In the literature, interference analysis for TDD-CDMA systems has been reported in [2]–[4]. In [2], the uplink interference, including the mobile-to-base and the base-to-base interference, was evaluated for the TDD-CDMA system with asymmetric traffic. It was concluded that the base-to-base interference (or called the cross-slot interference in this paper) will significantly decrease system capacity. In [3], the authors concluded that the cross-slot interference will occur if frames are not synchronized between adjacent cells. The authors in [3] suggested using an additional antenna protection between adjacent base stations or careful network planning to reduce the base-to-base cross-slot interference. In [4], antenna beamforming techniques were suggested to suppress the cross-slot interference for the TDD-CDMA system.

To minimize the cross-slot interference in the TDD-CDMA system, many code/time slot allocation schemes have been proposed, such as [5]–[9]. In [5], the authors proposed a time slot allocation scheme that can maximize radio resource utilization subject to the constraint of having a global switching point in a multiple cell environment. In [6], the authors concluded that a TDD-CDMA system using different switching points for different cells would outperform a system using the same switching point for all cells, but it was mentioned that finding the optimal switching points is a difficult task in a multi-cell environment. In [7], an interference-resolving algorithm was proposed to allow users who are close to their serving base stations to utilize opposite transmission directions in the same slot. In [8], [9], dynamic code/time slot allocation methods were suggested to minimize the cross-slot interference. However, the aforementioned works all assume that the TDD-CDMA system employs omnidirectional antennas.

This paper includes two major contributions. First, we develop an analytical framework to evaluate the interference problem of the TDD-CDMA system characterized by directional antennas and asymmetric traffics. To our knowledge, in the context of sectorized cellular structures, the interference issues in TDD-CDMA systems with asymmetric traffic have not been fully addressed in the literature. Second, we develop a resource allocation algorithm as applied to the "virtual cell" for a TDD-CDMA system. In [10], the concept of *virtual cell* was introduced, where a virtual cell consists of three neighboring sectors from three neighboring cells (e.g., sector S_1 of cell A, sector S_2 of cell C, and S_3 of cell D in Fig. 2). The similar concept was also proposed in [11] to reduce interference in FDD-CDMA systems. However, in the context of the TDD-CDMA system with asymmetric services, a resource allocation algorithm to explore the advantage of direction separation in the trisector cellular architecture has not been found in the literature. In this paper, we extend the work in [10], [11] to develop such a resource allocation algorithm to resolve the cross-slot interference for the TDD-CDMA system. The basic idea of the proposed algorithm can be described in two folds. On the one hand, by employing simple sector antennas at base stations (as shown in Fig. 2), we restrict the cross-slot interference within a cell coverage area. Applying the developed interference analysis framework, we will show that the interference between virtual cells can be suppressed due to the directivity of directional antennas. On the other hand, the cross-slot interference within a virtual cell can be resolved by a simple time slot allocation method. Hence, with trisector cellular architecture, the switching points of neighboring virtual cells can differ arbitrarily. In brief, taking advantage of this additional orthogonality from the direction separation of sector antennas, we propose a virtual cell-based interference-resolving algorithm to support asymmetric traffic services in TDD-CDMA systems.

The rest of this paper is organized as follows. In Section II, we analyze the uplink interference of the TDD-CDMA system with directional antennas and asymmetric services. Section III discusses the downlink interference analysis. Numerical results are provided in Section IV. In Section V, we describe the concept of virtual cells and present a code/time slot assignment algorithm for the sectorized TDD-CDMA system. By exploring the directionality of sectored antennas, the proposed algorithm just needs to avoid the cross-slot interference within local areas, thereby enabling the provision of flexible asymmetric traffic services. Simulation results are all provided in Section VI. Finally, conclusions are given in Section VII.

II. Uplink Interference Analysis for Base Stations

Fig. 3 shows the uplink interference scenario of the TDD-CDMA system. Without loss of generality, take sector S_{13} of cell 1 as an example. There are four kinds of entities that will cause the uplink interference:

- the mobile stations in the same sector S_{13}, denoted as $I^{(u)}_{\text{intra\_ms}}$;
- the mobile stations in the neighboring two sectors S_{11} and S_{12}, denoted as $I^{(u)}_{\text{intra\_ms\_}v}$;
- the mobile stations in the neighboring cells O_2 and O_3, denoted as $I^{(u)}_{\text{inter\_ms}}$;

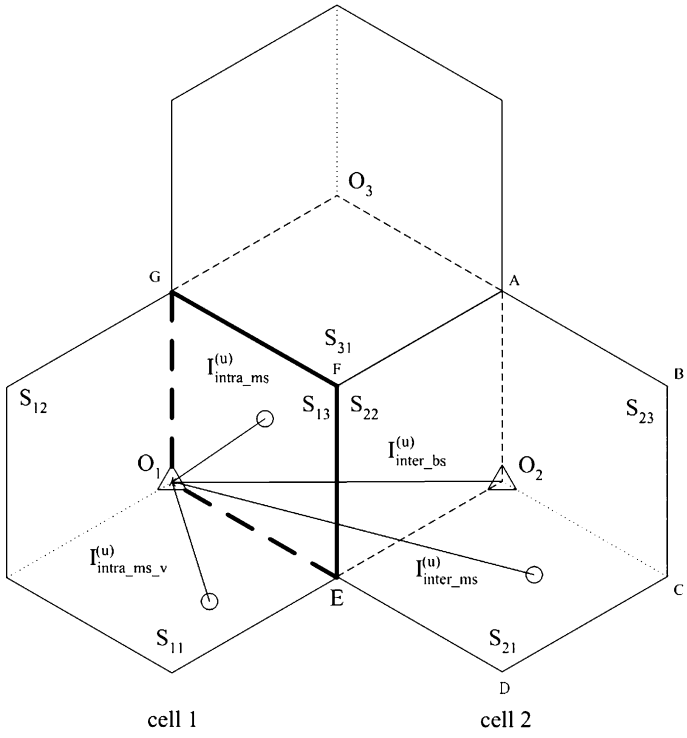

Fig. 3. Uplink interference scenario in the TDD-CDMA system.

- the base-to-base cross-slot interference from the six directional antennas in O_2 and O_3, denoted as $I^{(u)}_{\text{inter\_bs}}$.

A. Intracell Interference

Assume that N mobile stations are uniformly distributed in each cell. Let p_{ms} be the received power at a base station after power control. Then the interference from the mobile stations of the same sector (i.e., sector S_{13}) can be expressed as follows:

$$I^{(u)}_{\text{intra\_ms}} = \sum_{i=2}^{N/3} v_i p_{\text{ms}} \tag{1}$$

where v_i is the activity factor for user i.

Second, the interference from the mobile stations of sectors S_{11} and S_{12} within the same cell can be written as

$$I^{(u)}_{\text{intra\_ms\_}v} = v\rho\, p_{\text{ms}} \sum_{\chi\in\{11,12\}} \iint_{S_\chi} \frac{G_{13}(d_s,\theta_s)10^{\frac{\xi_s}{10}}}{G_\chi(d_s,\theta_s)10^{\frac{\xi_s}{10}}} \times \psi\left(G_{13}(d_s,\theta_s)10^{\frac{\xi_s}{10}}, G_\chi(d_s,\theta_s)10^{\frac{\xi_s}{10}}\right) dx\, dy \tag{2}$$

where $G_{13}(d_s,\theta_s)$ is the product of propagation loss and antenna gain for a user with a distance d_s and an angle θ_s to sector S_{13}, and ξ_s is the shadowing component, characterized by a Gaussian random variable with zero mean and standard deviation of σ_s dB. For example, if we consider the path loss model in [12] then

$$G_{13}(d_s,\theta_s) = \frac{h_b^2 h_m^2 G_b(\theta_s) G_m(\theta_m)}{d_s^4} \tag{3}$$

where h_b and h_m represent the antenna heights of base station and mobile terminal, respectively. Denote $G_b(\theta)$ and $G_m(\theta)$ the antenna gain betweens a base station and a mobile with the incident angle θ. Note that mobile terminals still use omnidirectional antennas (i.e., $G_m(\theta) = 1, 0 < \theta \le 360$). For ease of analysis, we set $h_b = 1$ and $h_m = 1$, and normalize the cell radius r_c to unity. Then the mobile stations density in each cell is $\rho = (\sqrt{3}N)/(6)(\text{mobiles/unit area})$. Let α and β be the path loss from two base stations to a mobile terminal. The function $\psi(\alpha,\beta)$ can be used to indicate whether $\alpha \le \beta$ or not, i.e.,

$$\psi(\alpha,\beta) = \begin{cases} 1, & \text{if } \alpha \le \beta \\ 0, & \text{otherwise.} \end{cases} \tag{4}$$

For example in (2), if $G_{12}(d_s,\theta_s)10^{(\xi_s)/(10)}$ is larger than $G_{13}(d_s,\theta_s)10^{(\xi_s)/(10)}$, then the mobile terminal is served by sector S_{12}; otherwise it will be served by sector S_{13}. Note that in (2), $G_{13}(d_s,\theta_s)10^{(\xi_s)/(10)}$ represents the link gain in sector S_{13} and $G_\chi(d_s,\theta_s)10^{(\xi_s)/(10)}$ denotes the compensation factor for the link attenuation during power control in sector S_χ, where $\chi \in \{11,12\}$. Here we adopt the same approach as in [13] to take average over v and ξ_s in (2). Accordingly, we obtain

$$E\left(I^{(u)}_{\text{intra\_ms\_}v}\right) = \rho p_{\text{ms}} E(v) \times \sum_{\chi\in\{11,12\}} \iint_{S_\chi} \frac{G_{13}(d_s,\theta_s)}{G_\chi(d_s,\theta_s)}\, dx\, dy. \tag{5}$$

B. Intercell Interference

Let $I^{(u)}_{\text{inter\_ms}}$ represent the interference from the mobile stations of cell 2. Then, $I^{(u)}_{\text{inter\_ms}}$ can be written as[1]

$$I^{(u)}_{\text{inter\_ms}} = v\rho p_{\text{ms}} \sum_{\chi\in\{21,22,23\}} \iint_{S_\chi} \frac{G_{13}(d_n,\theta_n)10^{\frac{\xi_n}{10}}}{G_\chi(d_s,\theta_s)10^{\frac{\xi_s}{10}}} \times \psi\left(G_{13}(d_n,\theta_n)10^{\frac{\xi_n}{10}}, G_\chi(d_s,\theta_s)10^{\frac{\xi_s}{10}}\right) dx\, dy, \tag{6}$$

where d_n and θ_n are the distance and the angle of the interfering mobile from cell 2; d_s and θ_s are the distance and the angle to the serving sectors from cell 2's standpoint; ξ_s and ξ_n are Gaussian random variables with zero mean and standard deviation of σ_s and σ_n, respectively. Note that $(\xi_n - \xi_s)$ in (6) is another Gaussian distributed random variable with zero mean and a standard deviation of $\sqrt{\sigma_n^2 + \sigma_s^2}$. Defining $\eta = (\ln 10)/(10)$ and taking the expected value of (6) with respect to v, ξ_n, and ξ_s, we obtain

$$E\left(I^{(u)}_{\text{inter\_ms}}\right) = \rho p_{\text{ms}} E(v) e^{\eta^2(\sigma_n^2+\sigma_s^2)/2} \cdot \sum_{\chi\in\{21,22,23\}} \iint_{S_\chi} \frac{G_{13}(d_n,\theta_n)}{G_\chi(d_s,\theta_s)} \times \left[1 - Q\left(\frac{\ln\left(\frac{G_\chi(d_s,\theta_s)}{G_{13}(d_n,\theta_n)}\right)}{\eta\sqrt{\sigma_n^2+\sigma_s^2}} - \eta\sqrt{\sigma_n^2+\sigma_s^2}\right)\right] dx\, dy \tag{7}$$

where $Q(x) = (1/\sqrt{2\pi}) \int_x^\infty e^{-t^2/2}\, dt$.

[1]Hereafter, the subscript s and n denote the variables associated with the serving cell and the neighboring cell, respectively. For example, ξ_n is the shadowing component of the neighboring cell, and ξ_s is the shadowing component of the serving cell.

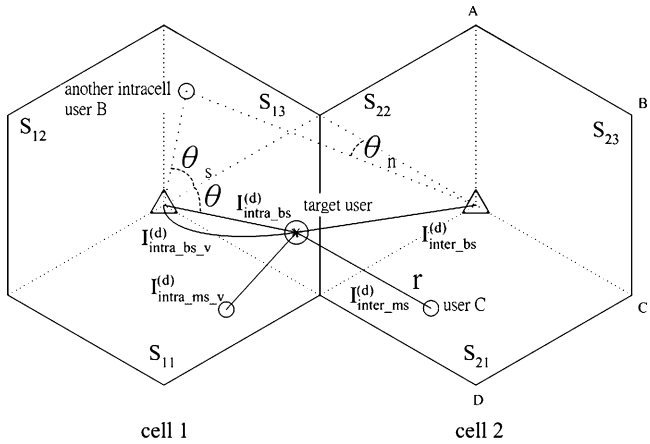

Fig. 4. Downlink interference scenario in the TDD-CDMA system.

C. Base-to-Base Cross-Slot Interference

The base-to-base interference $I^{(u)}_{\text{inter\_bs}}$ can be expressed as

$$I^{(u)}_{\text{inter\_bs}} = v\rho p_{\text{bs}} G_{13}(\theta_3) \sum_{\chi\in\{21,22,23\}} \iint\limits_{S_\chi} \frac{G_\chi(2r_c,\theta_\chi)10^{\frac{\xi_{\text{bs}}}{10}}}{G_\chi(d_s,\theta_s)10^{\frac{\xi_s}{10}}} \times\psi\left(G_{13}(d_n,\theta_n)10^{\frac{\xi_n}{10}}, G_\chi(d_s,\theta_s)10^{\frac{\xi_s}{0}}\right) dx\,dy \quad (8)$$

where p_{bs} is the received power at the mobile terminal after power control, $G_{13}(\theta_3)$ is the receiver antenna gain, $2r_c$ is the separation distance between two neighboring base stations, θ_χ is the angle of transmit antenna from cell 2 to sector S_{13}. Note that referring to Fig. 4, for serving a user in sectors $S_{21}, S_{22}, S_{23}, \theta_\chi$ is equal to $\angle DO_2O_1, \angle FO_2O_1, \angle BO_2O_1$, respectively. Furthermore, θ_3 in (8) is equal to $\angle FO_1O_2$. In (8), ξ_{bs} is the shadowing component between the two base stations with zero mean and standard deviation of σ_{bs}. Note that σ_{bs} is usually smaller than σ_n and σ_s because σ_{bs} is the shadowing component in the transmission path between two base stations. Taking average of (8) over v, ξ_n, ξ_s, and ξ_{bs}, we get

$$E\left(I^{(u)}_{\text{inter\_bs}}\right) = \rho p_{\text{bs}} E(v) e^{\eta^2(\sigma_s^2+\sigma_{\text{bs}}^2)/2} G_{13}(\theta_3) \times \sum_{\chi\in\{21,22,23\}} \iint\limits_{S_\chi} \frac{G_\chi(2r_c,\theta_\chi)}{G_\chi(d_s,\theta_s)} h\left(\frac{G_\chi(d_s,\theta_s)}{G_{13}(d_n,\theta_n)}\right) dx\,dy \quad (9)$$

where

$$h\left(\frac{G_\chi(d_s,\theta_s)}{G_{13}(d_n,\theta_n)}\right) = \int\limits_{-\infty}^{\infty} \frac{e^{-t^2}}{\sqrt{\pi}} Q\left(\sigma_s\eta + \frac{\sqrt{2}\sigma_n t - 10\log_{10}\left(\frac{G_\chi(d_s,\theta_s)}{G_{13}(d_n,\theta_n)}\right)}{\sigma_s}\right) dt. \quad (10)$$

To facilitate the computation of the numerical results in (9), we can apply the Hermite polynomial method of [14]. The Hermite approximation method can transfer an integration into a summation, i.e.,

$$\int\limits_{-\infty}^{\infty} f(t)\exp(-t^2)\,dt = \sum_{i=1}^{k} w_i f(t_i) + R_k \quad (11)$$

where t_i and w_i are predetermined roots and weighting factors defined in [14]. Hence, we can simplify the computation of $h(\cdot)$ in (9) by applying (11) with

$$f(t) = \frac{1}{\sqrt{\pi}} Q\left(\sigma_s\eta + \frac{\sqrt{2}\sigma_n t - 10\log_{10}\left(\frac{G_\chi(d_s,\theta_s)}{G_{13}(d_n,\theta_n)}\right)}{\sigma_s}\right). \quad (12)$$

III. Downlink Interference Analysis for Mobile Terminals

Now we analyze the downlink interference as shown in Fig. 4. We focus on user A served by sector S_{13} of cell 1. There are five kinds of interference sources for user A:

- the interfering signals $I^{(d)}_{\text{intra\_bs}}$ from the same antenna S_{13}, but targeted at different users other than user A;
- the interfering signals $I^{(d)}_{\text{intra\_bs\_}v}$ from the neighboring antennas S_{11} and S_{12};
- the interfering signals $I^{(d)}_{\text{inter\_bs}}$ from the three directional antennas in O_2;
- the interfering signals $I^{(d)}_{\text{intra\_ms\_}v}$ from the mobile stations in the neighboring sectors S_{11} and S_{12};
- the interfering signals $I^{(d)}_{\text{inter\_ms}}$ from the mobile stations in the neighboring cell O_2.

A. Intracell Interference

1) The Same Sector Case: For the same antenna of the serving base station, we express $I^{(d)}_{\text{intra\_bs}}$ as

$$I^{(d)}_{\text{intra\_bs}} = v\rho\, p_{\text{bs}} \Phi_{S_{13}} \iint\limits_{S_{13}} \frac{G_{13}(d,\theta)10^{\frac{\xi_i}{10}}}{G_{13}(d_s,\theta_s)10^{\frac{\xi_s}{10}}} \times\psi\left(G_{22}(d_n,\theta_n)10^{\frac{\xi_n}{10}}, G_{13}(d_s,\theta_s)10^{\frac{\xi_s}{10}}\right) dx\,dy \quad (13)$$

where $\Phi_{S_{13}}$ is the orthogonality factor between the codes used in the same sector $0 \le \Phi_{S_{13}} \le 1$. In (13), as shown in Fig. 4, d and θ represent the distance and the angle of the target mobile terminal A to the base station; d_s and d_n represent the distance from another intracell user B to the serving cell and that to the neighboring cell, respectively; ξ_i is the shadowing component between the base station and the interfered mobile terminal A, which is characterized by a Gaussian random variable with zero mean and a standard deviation of σ_i. Taking average over v, ξ_n, ξ_s, and ξ_i, we can obtain

$$E\left(I^{(d)}_{\text{intra\_bs}}\right) = \rho p_{\text{ms}} E(v) e^{\eta^2(\sigma_s^2+\sigma_i^2)/2} \times \iint\limits_{S_\chi} \Phi_{S_{13}} \frac{G_{13}(d,\theta)}{G_{13}(d_s,\theta_s)} h\left(\frac{G_{13}(d_s,\theta_s)}{G_{22}(d_n,\theta_n)}\right) dx\,dy \quad (14)$$

where $h(\cdot)$ is the same as in (10).

2) The Neighboring Sector Case: The interference $I^{(d)}_{\text{intra\_bs\_}v}$ from the neighboring sectors' antennas of the serving cell can be expressed as

$$I^{(d)}_{\text{intra\_bs\_}v} = v\rho p_{\text{bs}} \sum_{\chi\in\{11,12\}} \iint_{S_\chi} \frac{G_\chi(d,\theta)10^{\frac{\xi_i}{10}}}{G_\chi(d_s,\theta_s)10^{\frac{\xi_s}{10}}} \Phi_{S_\chi S_{13}} \times \psi\left(G_{13}(d_n,\theta_n)10^{\frac{\xi_n}{10}}, G_\chi(d_s,\theta_s)10^{\frac{\xi_s}{10}}\right) dx\,dy \quad (15)$$

where $\Phi_{S_\chi S_{13}}$ is the orthogonality factor between the codes in sectors S_χ and S_{13}. Noteworthily, by taking advantage of the separation of sector antennas, the orthogonality factor $\Phi_{S_\chi S_{13}} < 1$ in most sector antenna cases, while in the omnidirectional antenna case $\Phi_{S_\chi S_{13}} = 1$. By taking average with respect to v, ξ_n, ξ_s, and ξ_i, we get

$$E\left(I^{(d)}_{\text{intra\_bs\_}v}\right) = \rho p_{\text{bs}} E(v) e^{\eta^2(\sigma_s^2+\sigma_i^2)/2} \times \sum_{\chi\in\{11,12\}} \iint_{S_\chi} \frac{G_\chi(d,\theta)}{G_\chi(d_s,\theta_s)} \Phi_{S_\chi S_{13}} h\left(\frac{G_\chi(d_s,\theta_s)}{G_{13}(d_n,\theta_n)}\right) dx\,dy. \quad (16)$$

B. Intercell Interference

The downlink interference from the neighboring base station, $I^{(d)}_{\text{inter\_bs}}$, can be written as

$$I^{(d)}_{\text{inter\_bs}} = v\rho p_{\text{bs}} \sum_{\chi\in\{21,22,23\}} \iint_{S_\chi} \frac{G_\chi(d,\theta)10^{\frac{\xi_i}{10}}}{G_\chi(d_s,\theta_s)10^{\frac{\xi_s}{10}}} \times \Phi_{S_\chi S_{13}} \psi\left(G_{13}(d_n,\theta_n)10^{\frac{\xi_n}{10}}, G_\chi(d_s,\theta_s)10^{\frac{\xi_s}{10}}\right) dx\,dy. \quad (17)$$

Because of the protection from the directivity of sector antennas, $\Phi_{S21S_{13}}$ and $\Phi_{S_{23}S_{13}}$ can be any values less than one as in (15). However, $\Phi_{S_{22}S_{13}}$ should be chosen as small as possible due to the lack of antenna separation. By taking average with respect to v, ξ_n, ξ_s, and ξ_i, we obtain

$$E\left(I^{(d)}_{\text{inter\_bs}}\right) = \rho p_{\text{bs}} E(v) e^{\eta^2(\sigma_s^2+\sigma_i^2)/2} \times \sum_{\chi\in\{21,22,23\}} \iint_{S_\chi} \frac{G_\chi(d,\theta)}{G_\chi(d_s,\theta_s)} \Phi_{S_\chi S_{13}} h \times \left(\frac{G_\chi(d_s,\theta_s)}{G_{13}(d_n,\theta_n)}\right) dx\,dy \quad (18)$$

where $h(\cdot)$ is the same as (10).

C. Mobile-to-Mobile Cross-Slot Interference

1) The Same Cell Case: For the downlink interference $I^{(d)}_{\text{intra\_ms\_}v}$ from the mobile stations of the neighboring sector, because the omnidirectional antenna is used for mobile terminals, we ignore the antenna gain and express $I^{(d)}_{\text{intra\_ms\_}v}$ as

$$I^{(d)}_{\text{intra\_ms\_}v} = v\rho p_{\text{ms}} \sum_{\chi\in\{11,12\}} \iint_{S_\chi} \frac{(r^{-4})10^{\frac{\xi_{\text{ms}}}{10}}}{G_\chi(d_s,\theta_s)10^{\frac{\xi_s}{10}}} \times \psi\left(G_{13}(d_s,\theta_x)10^{\frac{\xi_s}{10}}, G_\chi(d_s,\theta_s)10^{\frac{\xi_s}{10}}\right) dx\,dy \quad (19)$$

where r is the distance between the mobile terminal C in cell 2 and the interfered mobile B in cell 1, and ξ_{ms} is the shadowing component between the two mobile terminals. Taking average over v, ξ_s, and ξ_{ms}, we obtain

$$E\left(I^{(d)}_{\text{intra\_ms\_}v}\right) = \rho p_{\text{ms}} E(v) e^{\eta^2(\sigma_s^2+\sigma_{\text{ms}}^2)/2} \times \sum_{\chi\in\{11,12\}} \iint_{S_\chi} \frac{(r^{-4})}{G_\chi(d_s,\theta_s)}\, dx\,dy. \quad (20)$$

2) The Other Cell Case: We can express the cross-slot interference from mobile stations of the other cells $I^{(d)}_{\text{inter\_ms}}$ as

$$I^{(d)}_{\text{inter\_ms}} = v\rho p_{\text{ms}} \sum_{\chi\in\{21,22,23\}} \iint_{S_\chi} \frac{(r^{-4})10^{\frac{\xi_{\text{ms}}}{10}}}{G_\chi(d_s,\theta_s)10^{\frac{\xi_s}{10}}} \times \psi\left(G_{13}(d_n,\theta_n)10^{\frac{\xi_n}{10}}, G_\chi(d_s,\theta_s)10^{\frac{\xi_s}{10}}\right) dx\,dy. \quad (21)$$

Taking average over v, ξ_n, ξ_s, and ξ_{ms}, we obtain

$$E\left(I^{(d)}_{\text{inter\_ms}}\right) = \rho p_{\text{ms}} E(v) e^{\eta^2(\sigma_s^2+\sigma_{\text{ms}}^2)/2} \times \sum_{\chi\in\{21,22,23\}} \iint_{S_\chi} \frac{(r^{-4})}{G_\chi(d_s,\theta_s)} h\left(\frac{G_\chi(d_s,\theta_s)}{G_{13}(d_n,\theta_n)}\right) dx\,dy. \quad (22)$$

Note that the computation of (14), (18), and (22) can be simplified by using the Hermite polynomial approach introduced in (11).

IV. Effect of Directional Antenna

A. Uplink Interference

In this section, we present numerical results based on the interference analysis in Sections II and III. Consider the interference scenario as shown in Fig. 3. Let the centers of cell 1 and cell 2 be located at (0, 0) and (2 km, 0), respectively, where cell radius r_c equal to 1 km. According to (7) and (9), we calculate the intercell interference of the TDD-CDMA system with omnidirectional and directional base station antennas. In our simulation, we consider three different shadowing components: $\sigma_s = 9$ dB, $\sigma_n = 8$ dB, and $\sigma_{\text{bs}} = 3$ dB, where σ_s and σ_n are the standard deviations of the shadowing component between a mobile and a serving base station, and that between a mobile and the neighboring interfering base station, respectively; and σ_{bs} is that between two base stations.

Fig. 5 shows the uplink base-to-base cross-slot interference $I^{(u)}_{\text{inter\_bs}}$ for the TDD-CDMA system with directional antennas. In the figure, points A, B, C, and D stand for the corners of cell 2 in Fig. 3. According to (9), we calculate the base-to-base interference when a mobile of cell 2 moves to different locations within the cell. The values in the z axis represent the base-to-base interference normalized to p_{bs}, where $p_{\text{bs}} = -97$ dBm is the downlink received power at a mobile terminal after power control. We find that if that user is located at points B, C, or D of cell 2, the base-to-base interference from cell 2 to cell 1 is reduced due to the separation of sector antennas. When the base station of cell 2 serves a particular mobile being located at point A, the base-to-base cross-slot interference will be amplified due to the directional antenna gain. Hence, using

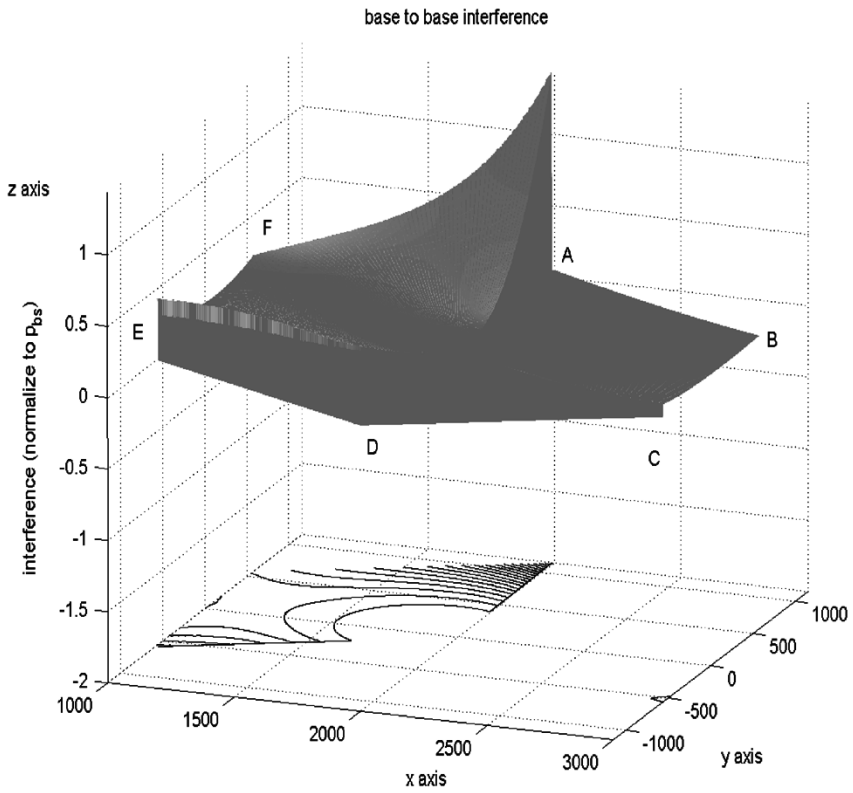

Fig. 5. Uplink base-to-base interference from cell 2 to cell 1 with directional antenna, where $p_{\rm bs}$ is the downlink received power at a mobile in sector S_{13}, and points A, B, C, and D represent the corners of cell 2 in Fig. 3.

directional antennas in a trisector cellular system can restrict the strong base-to-base interference into a hexagon area labeled with A-O_2-E-O_1-G-O_3 as shown in Fig. 3. Consequently, the base-to-base cross-slot interference can be possibly avoided by just coordinating the switching points of downlink and uplink bandwidth ratio in only three sectors for the TDD-CDMA with the trisector cellular system.

For comparison, Fig. 6 shows the base-to-base cross-slot interference of the TDD-CDMA system with omnidirectional antennas employed at base stations. One can find that cell 1 can very likely receive severe base-to-base cross-slot interference from cell 2 when a mobile terminal of cell 2 is located at the cell boundary, e.g., points A, B, C, and D of cell 2. Thus, unlike the trisector TDD-CDMA cellular system, the base-to-base cross-slot interference in the omnidirectional cellular system will influence all the surrounding cells. Therefore, it is necessary to globally control the switching points in every cell.

Fig. 7 shows the mobile-to-base interference $I^{(u)}_{\rm inter\_ms}$ of (6) for the TDD-CDMA system with directional antennas. The values in the z axis represent the mobile-to-base interference normalized to $p_{\rm ms}$, where $p_{\rm ms} = -112$ dBm is the uplink received power at the base station after power control. One can find that the shorter the distance to the serving base station, the less the interference to the neighboring cell. This is because at a further distance, such as point B, the mobile terminal needs to transmit higher power to compensate path loss and shadowing. Besides, because the mobile terminal still uses omnidirectional antenna, the mobile-to-base interference in a system with omnidirectional antennas is similar to the system with directional antennas. Due to the length limitation of the paper, we will not show the result here.

B. Downlink Interference

Now, we investigate the performance differences between the trisector TDD-CDMA cellular system and the omnidirectional cellular system in terms of downlink interference. We consider the interference scenario as shown in Fig. 4. Let the mobile be located at (0.4 km, 0) of cell 1. We evaluate the received inter-cell interference of the TDD-CDMA system for the cases with omnidirectional antennas and directional antennas according to (18) and (22). Denote $\sigma_{\rm ms}$ and σ_i as the standard deviation of shadowing component from the observed mobile to a nearby mobile and that to a base station, respectively. In our analysis, we adopt $\sigma_{\rm ms} = 10$ dB and $\sigma_i = 8.5$ dB.

By evaluating (18), Fig. 8 shows the base-to-mobile interference in the TDD-CDMA system with directional antennas. In the figure, points A, B, C, and D represent the corners of sectors S_{22}, S_{23}, and S_{21} in Fig. 4. One can see that only sector S_{22} of cell 2 will cause serious interference to cell 1, while the other sectors of cell 2 will not yield strong interference. This result indicates that in the trisector cellular system we should set the same downlink and uplink bandwidth ratio in sector S_{22} of cell 2 and sector S_{13} of cell 1. We define an area with three adjacent diamond-shaped sectors belonging to three different base stations as a *virtual cell*, which will be discussed in Section V.

Fig. 9 shows the base-to-mobile interference $I^{(d)}_{\rm inter\_bs}$ in a system employing the omnidirectional base station antenna. As shown in the figure, when the neighboring base station is serving

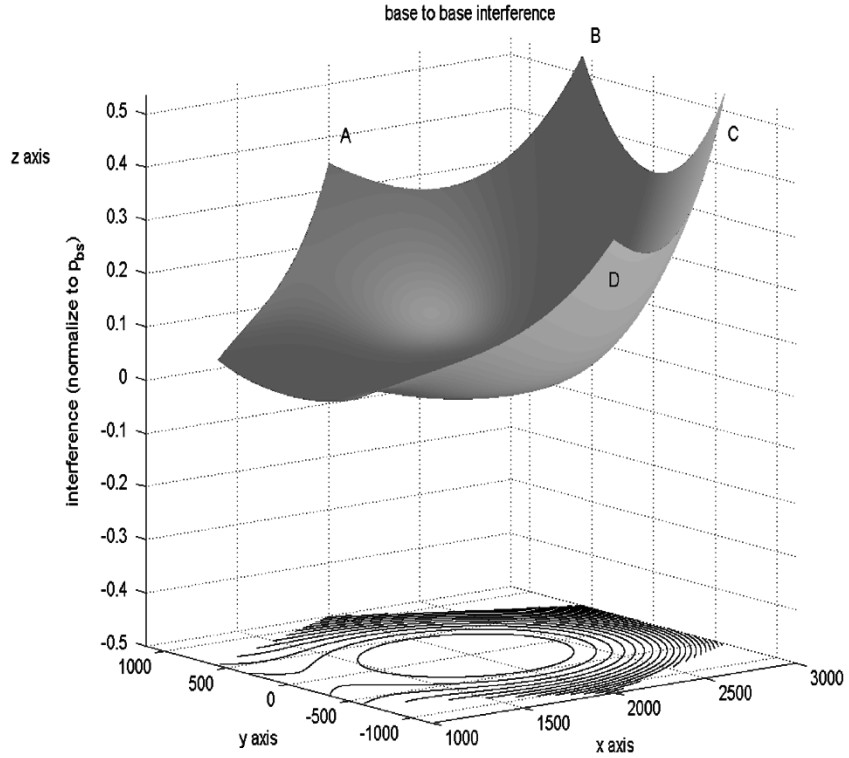

Fig. 6. Uplink base-to-base interference from cell 2 to cell 1 with omnidirectional antenna, where $p_{\rm bs}$ is the downlink received power at a mobile in sector S_{13}, and points A, B, C, and D represent the corners of cell 2 in Fig. 3.

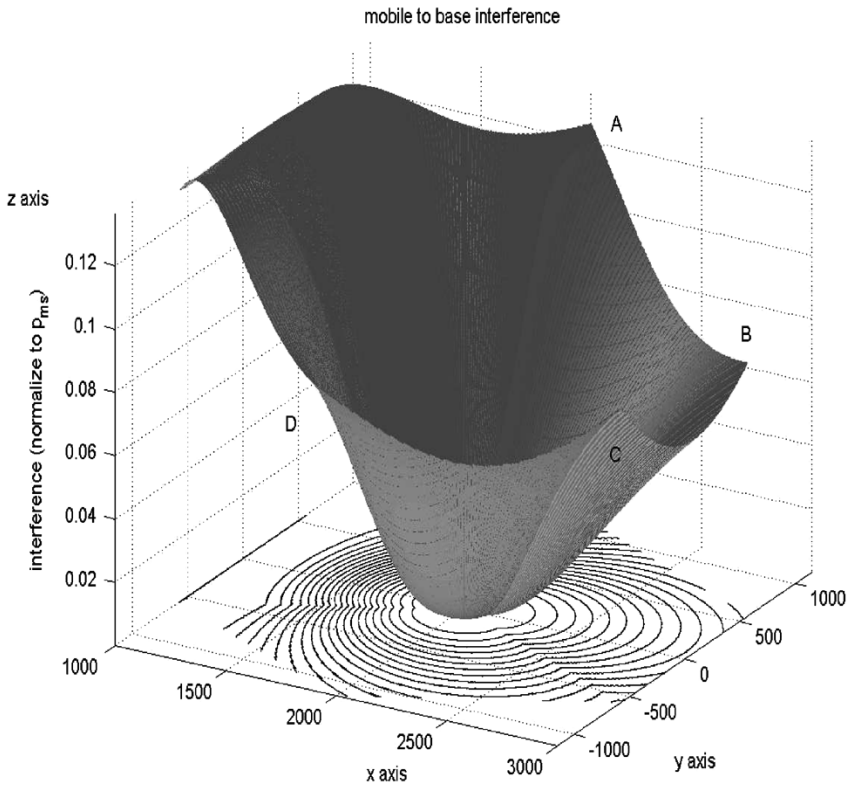

Fig. 7. Uplink mobile-to-base interference from cell 2 to cell 1 with trisector directional antenna, where $p_{\rm bs}$ is the downlink received power at a mobile in sector S_{13}, and points A, B, C, and D represent the corners of cell 2 in Fig. 3.

a mobile station at a longer distance, the signal from the base station will cause very strong interference to the downlink reception quality at the target mobile station. For example, consider point B at cell 2. Unlike the small interference in the directional antennas case (i.e., $0.2\,p_{\rm bs}$), the interference $I^{(d)}_{\rm inter\_bs}$ to mobiles in cell 1 is $6.8\,p_{\rm bs}$.

By evaluating (22), Fig. 10 shows the mobile-to-mobile cross-slot interference $I^{(d)}_{\rm inter\_ms}$ from cell 2 in the TDD-CDMA

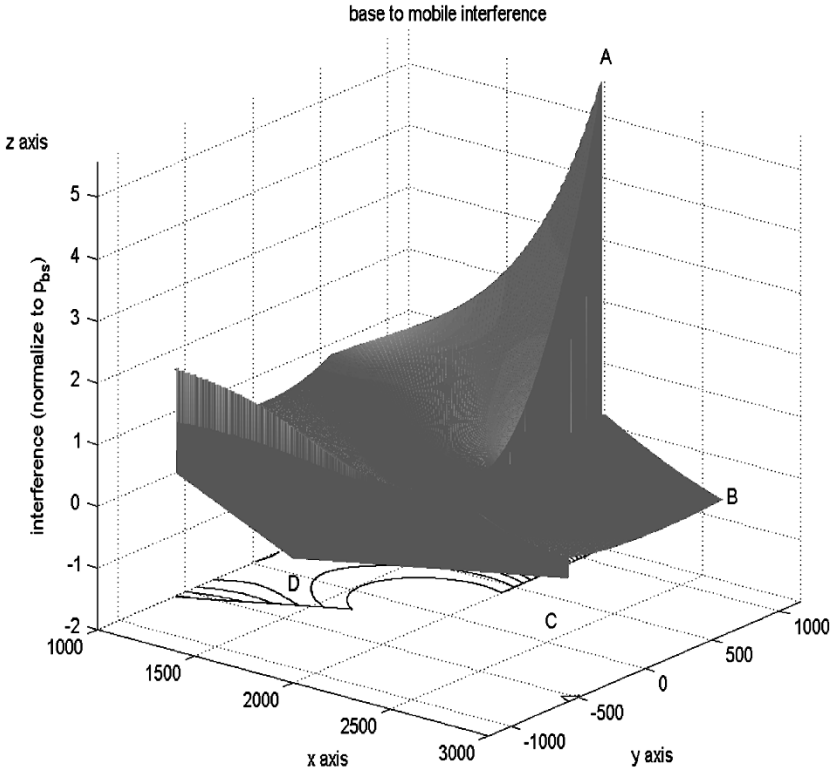

Fig. 8. Downlink base-to-mobile interference from cell 2 to cell 1 with directional antenna, where $p_{\rm bs}$ is the downlink received power at a mobile in sector S_{13}, and points A, B, C, and D represent the corners of cell 2 in Fig. 4.

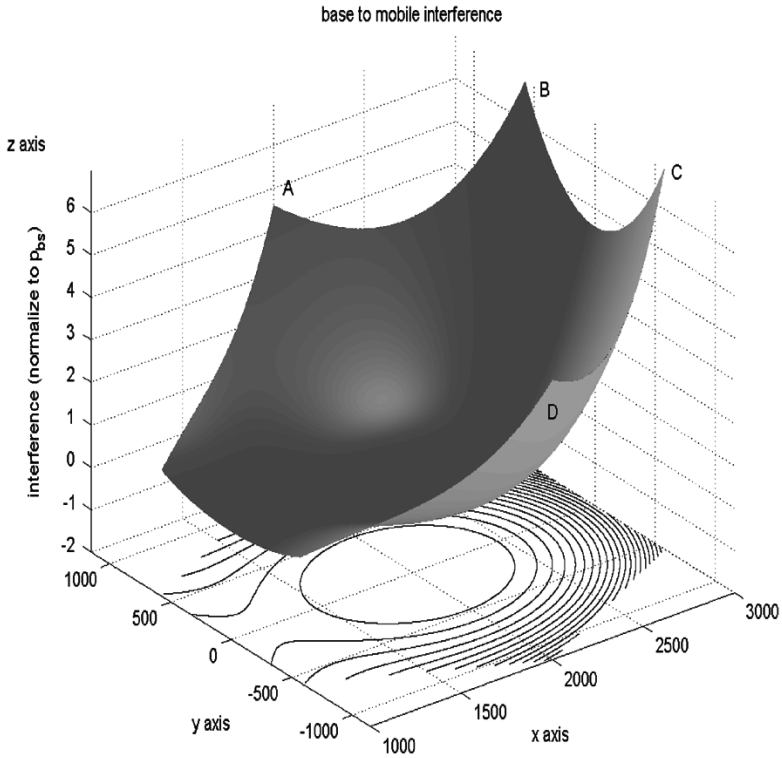

Fig. 9. Downlink base-to-mobile interference from cell 2 to cell 1 with omnidirectional antenna, where $p_{\rm bs}$ is the downlink received power at a mobile in sector S_{13}, and points A, B, C, and D represent the corners of cell 2 in Fig. 4.

system with directional antennas. If the transmission directions of two neighboring cells are opposite during a particular time slot, only the mobile station closer to the cell boundary of cell 2 will cause stronger cross-slot interference to a nearby mobile in cell 1. For the omnidirectional cellular system, we obtain a similar result of mobile-to-mobile cross-slot interference, which is not shown here. We find that the cross-slot interference level in the omnidirectional case is slightly larger than that in

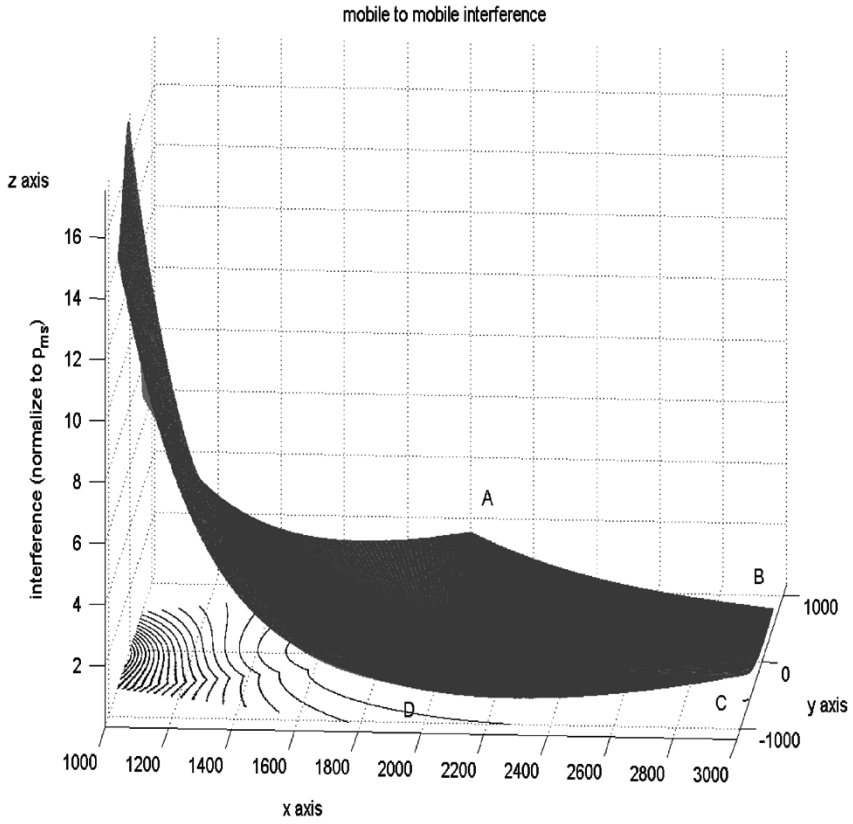

Fig. 10. Downlink mobile-to-mobile interference from cell 2 to cell 1 with directional antenna, where $p_{\rm bs}$ is the downlink received power at a mobile in sector S_{13}, and points A, B, C, and D represent the corners of cell 2 in Fig. 4.

the directional antenna case because the transmission power from a mobile station in the omnidirectional cellular system is greater than that in the trisector cellular system due to the smaller antenna gain.

C. Verification

To verify our analysis, the left part of Table I illustrates the uplink interference obtained from both analysis and simulation. By evaluating (7) and (9) according to the Hermite polynomial approach, we find that the estimated interference of the TDD-CDMA system is close to simulation results. Noteworthily, the base-to-base interference (i.e., $I^{(u)}_{\rm inter\_bs}$) is higher than the interference from mobile terminals $I^{(u)}_{\rm inter\_ms}$ because the transmission power of a base station is higher than that of a mobile station, i.e., $p_{\rm bs} > p_{\rm ms}$.

In the right part of Table I, we show the analytical and simulation results for downlink interference. The analysis results are obtained from (18) and (22). One can see that the cross-slot interference $I^{(d)}_{\rm inter\_ms}$ can be quite significant as the interfering mobile terminals are close to the cell boundary although $p_{\rm bs}$ is 15 dB larger than $p_{\rm ms}$. Thus, we are motivated to design a resource allocation scheme to coordinate the switching points within a virtual cell, i.e., an area with the three adjacent sectors belonging to three different base stations. By doing so, we can avoid the mobile-to-mobile cross-slot interference for the TDD-CDMA system.

From the above observations, we find that the problem of setting switching point can be simplified from the complicated global control in the whole system to the simpler local control in only three sectors within a virtual cell. In the next section, we will present a code/time slot allocation scheme for the TDD-CDMA system to explore this advantage inherently in directional antenna.

TABLE I
COMPARISON OF ANALYSIS AND SIMULATION FOR UPLINK AND DOWNLINK INTERFERENCE

Uplink

$I^{(u)}_{inter\_ms}$	Simulation	7.0999 (p_{ms})
	Analysis	6.9223 (p_{ms})
	Difference	2.5652%
$I^{(u)}_{inter\_bs}$	Simulation	7.6744 (p_{bs})
	Analysis	7.4540 (p_{bs})
	Difference	2.9571%

Downlink

$I^{(d)}_{inter\_ms}$	Simulation	158.1143 (p_{ms})
	Analysis	148.7765 (p_{ms})
	Difference	6.2764%
$I^{(d)}_{inter\_bs}$	Simulation	30.5988 (p_{bs})
	Analysis	28.9837 (p_{bs})
	Difference	5.5726%

V. VIRTUAL CELL-BASED CODE/TIME RESOURCE ALLOCATION ALGORITHM

A. Concept of Virtual Cell

In the previous section, we find that with directional antennas employed at base stations, it is possible to relax the limitation

of forcing neighboring cells to have the same uplink and downlink transmission directions required in the system with omnidirectional antennas. Consider the trisector cellular system as shown in Fig. 2, the uplink transmission of a user terminal at sector $\mathbf{S_2}$ of cell **A** will no longer be influenced by sector $\mathbf{S_2}$ of cells **B**, **C**, **D**, and **H**. This is because the location of cell **A** is behind the back lobe of cells B, C, D, and H. For the uplink transmission of the same user terminal, the interference from cells **F** and **G** is also lighter than that in the case with omnidirection antenna because these interfering sources face the back lobe of sector $\mathbf{S_2}$ of cell **A**. Hence, we find that the interference including the cross-slot interference in the trisector cellular architecture can be restricted in an area composing of three adjacent diamond-shaped sectors each of which belongs to three different cells. We call such an area in the trisector cellular system the virtual cell. The shaped area in Fig. 2 shows an example of a virtual cell, which is composed of sector $\mathbf{S_3}$ of cell **C**, sector $\mathbf{S_2}$ of cell **D**, and sector $\mathbf{S_1}$ of cell **F**.

B. Code/Time Slot Assignment Scheme

The main purpose of proposed *virtual cell*-based code/time slot assignment scheme is to set the same switching point in the three sectors of each virtual cell, while neighboring virtual cells can have different setting on their switching point. The switching point is used to divide the time frame into two groups for uplink and downlink transmissions. It also can be treated as the uplink-to-downlink ratio of a time frame. Specifically, the uplink slot assignment begins from the beginning of the frame until the switching point, and downlink slot assignment begins from the end of the frame to the switching point. Each virtual cell can support the same number of users as a regular cell in the system with omnidirectional antennas, and the radio resources are shared within the three sectors in a virtual cell. Thus, to apply the virtual cell-based code/time slot assignment scheme in the TDD/CDMA system, we consider the traffic load in every diamond-shaped sector rather than a hexagon-shaped cell.

Fig. 11 shows one probable scenario, where U_i, and D_i denotes the required uplink/downlink code/time slots of sector i in the uplink and those in the downlink, respectively. We define $L(\mathrm{SP})$ as the function of unsatisfied traffic requirements, and SP is the switching point, which is an integer over the interval [0, 8]. For exmple, if we set SP equal to $0, L(0)$ will equal to $U_1+U_2+U_3 = 10$ due to no uplink slot is allocated. On the contrary, if we set SP equal to $8, L(8)$ will equal to $D_1+D_2+D_3 = 9$. Thus, we may find the minimum unsatisfied requirements by substituting all possible switching point setting into $L(\cdot)$. However, if $\mathrm{Max}(U_1, U_2, U_3) + \mathrm{Max}(D_1, D_2, D_3) < 8$, all integers over the interval $[\mathrm{Max}(U_1, U_2, U_3), 8-\mathrm{Max}(D_1, D_2, D_3)]$ minimize the unsatisfied requirement.

After switching points among each virtual cell is set, the uplink slot assignment begins from the beginning of the frame until the switching point, and downlink slot assignment begins from the end of the frame to the switching point. When there is a new mobile arrival, the system will allocate multicodes within one time slot, or in the next time slot if necessary. If the remaining available code/time slots is not enough, this request from the mobile will be blocked. As shown in Fig. 12, we assume that

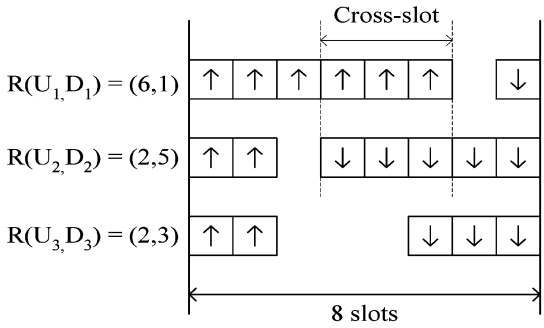

Fig. 11. An example for setting the switching point among the virtual cell.

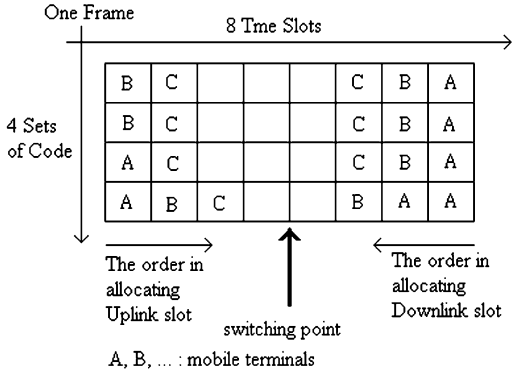

Fig. 12. The scheme of time slot allocation.

a frame contains eight time slots during each of which four orthogonal codes can be assigned to a user. In this example, mobile A requests two uplink time slots and five downlink time slots. Then we assign two codes in the first time slot for the uplink transmission and five codes in the last two time slots for the downlink transmission. When mobile B arrives and requests three uplink slots and four downlink slots, the remaining two codes in the first time slot and the one code in the second time slot are allocated for uplink transmissions. The remaining three codes in the seventh time slot and one code in the sixth time slot are allocated for downlink transmissions.

VI. Simulation Results

Based on the proposed code/time slot assignment scheme, we simulate the signal-to-interference ratio (S/I) and call blocking performance in a TDD-CDMA system with 19 cells as shown in Fig. 2. To demonstrate the advantage of using directional antennas in TDD-CDMA system, four kinds of slot assignment schemes are compared:

- Scheme I: the global control on the switching point setting in the TDD-CDMA system with omnidirectional antennas;
- Scheme II: the distributed control on the switching point setting in the TDD-CDMA system with omnidirectional antennas, where every cell has different switching point setting;
- Scheme III: the proposed virtual cell-based slot allocation algorithm in the trisector TDD-CDMA cellular system;
- Scheme IV: the sector-by-sector based switching point setting in the trisector TDD-CDMA cellular system.

TABLE II
UPLINK AND DOWNLINK TRAFFIC REQUIREMENT IN EACH SECTOR OF FIG. 2

	Sector 1		Sector 2		Sector 3	
Cell	Required Uplink Slot	Required Downlink Slot	Required Uplink Slot	Required Downlink Slot	Required Uplink Slot	Required Downlink Slot
A	2	5	2	6	2	4
B	2	5	2	3	2	6
C	5	2	2	5	3	3
D	2	4	2	2	3	4
E	5	3	2	4	3	2
F	2	5	3	5	2	5
G	2	4	2	6	2	5
H	4	2	2	5	2	3
I	2	4	2	4	2	5
J	3	3	2	3	2	2
K	3	4	4	3	4	2
L	5	2	2	5	2	4
M	3	5	2	4	2	5
N	2	5	2	4	2	5
O	2	3	2	4	2	4
P	2	5	3	3	4	3
Q	5	2	3	4	4	3
R	4	2	5	2	2	5
S	2	4	3	5	2	4

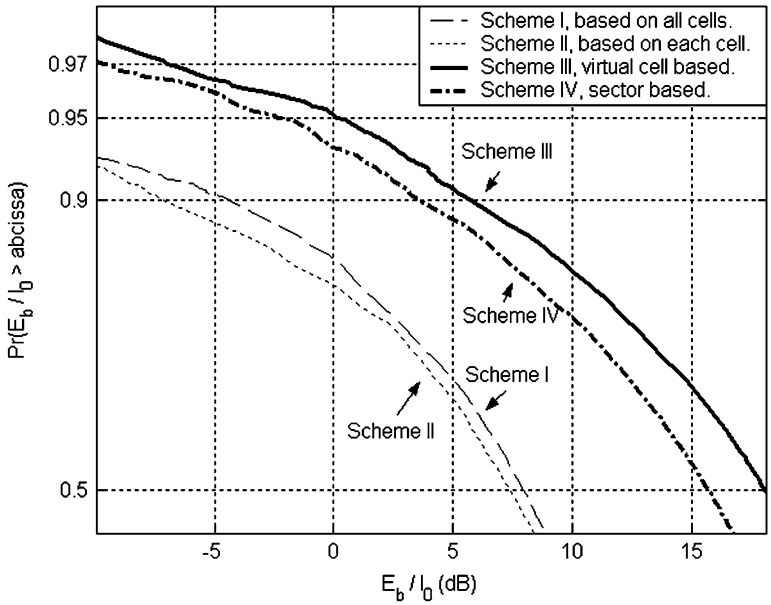

Fig. 13. Uplink E_b/I_0 performance of slot allocation schemes in both omnidirectional and trisector cellular system, where Scheme I is the global setting in omni case, Scheme II is the local setting in omni case, Scheme III is the proposed virtual cell-based case, and Scheme IV is the sector based setting in directional case.

In our simulation, we evaluate both the bit energy to the interference density ratio E_b/I_0 and call blocking performances in the TDD-CDMA system with directional antennas and those with omnidirectional antennas, where $E_b/I_{0(\mathrm{dB})} = S/I_{(\mathrm{dB})} + \mathrm{PG}_{(\mathrm{dB})}$. Here we consider a processing gain $\mathrm{PG} = 10$ dB. Assume that the up/downlink bandwidth requirements in each sector are different as shown in Table II. Let each cell have the same number of codes and time slots, i.e., a frame containing eight time slots and nine sets of orthogonal codes. Furthermore, we assume that every virtual cell is allowed to manage its own radio resource, To eliminate the boundary effect in simulation, we also adopt the wrap-around technique in a 19-cell environment.

Fig. 13 compares the uplink E_b/I_0 performance of the four aforementioned slot assignment schemes. In the figure, there are two groups of curves. The curves in the right part are the E_b/I_0 performance for a system with directional antennas, and the left part is that for a system with omnidirectional antennas. It is obvious that both Schemes III and IV with directional antennas outperform Schemes I and II with omnidirectional antennas. Focusing on the curves of Schemes III and IV, we find that the E_b/I_0 performance of Scheme III is slightly better than Scheme IV. This is because the intercell interference is smaller in Scheme III. Though in Scheme IV the intercell interference can also be restricted in a small area, if the switching point settings of the three neighboring sectors in a virtual cell are different, the cross-slot interference among the three sectors can still degrade the 90th percentile of E_b/I_0 performance by 1.5 dB compared to Scheme III. Because of the same reason, the

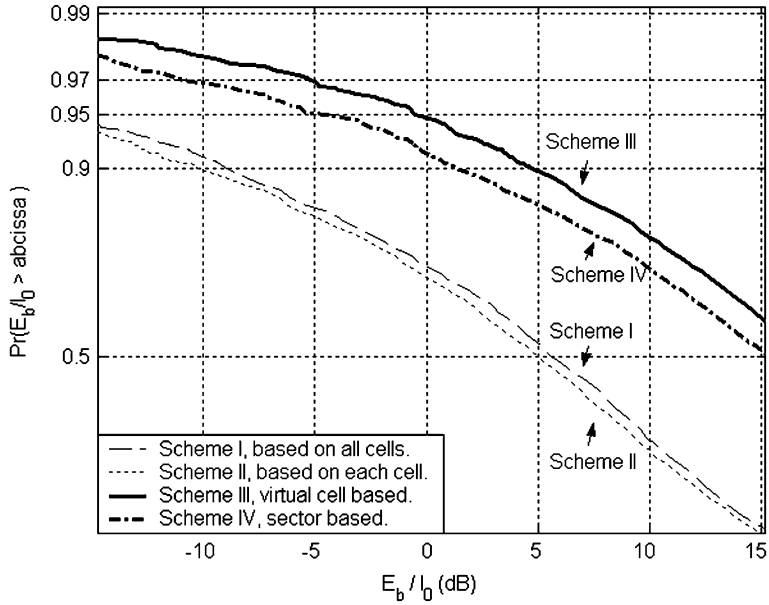

Fig. 14. Downlink E_b/I_0 performance of slot allocation schemes in both omnidirectional and trisector cellular system, where Scheme I is the global setting in omni case, Scheme II is the local setting in omni case, Scheme III is the proposed virtual cell-based case, and Scheme IV is the sector based setting in directional case.

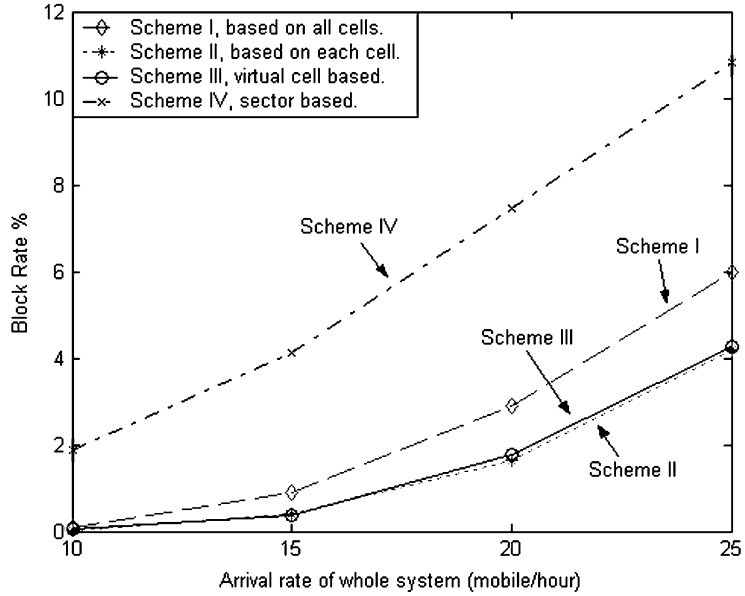

Fig. 15. The blocking rate comparison of TDD-CDMA system between four different setting, where Scheme I is the global setting in omni case, Scheme II is the local setting in omni case, Scheme III is the proposed virtual cell-based case, and Scheme IV is the sector based setting in directional case.

E_b/I_0 performance of Scheme I (i.e., the omnidirectional antenna case with the global control on the switching point setting) is better than Scheme II (i.e., the omnidirectional antenna case with local setting). Thus, in the system with omnidirectional antennas, it may be necessary to set the same switching point in all cells to avoid cross-slot interference.

Fig. 14 compares the downlink E_b/I_0 performances of the aforementioned four time slot allocation schemes. In the figure, one can see that the E_b/I_0 performances of Schemes III and IV (the curves in the right part) outperform Schemes I and II. For example, the 90th percentiles of E_b/I_0 for Schemes III and IV are 5 and 1.5 dB, respectively, while the 90th percentiles of E_b/I_0 for Schemes I and II are -9 and -10 dB. The performance improvements of Schemes III and IV over Schemes I and II are explained as follows. The major cross-slot interfering signals are from all the surrounding six cells in Schemes I and II, while there are only three sectors within a virtual cell causing cross-slot interference in Schemes III and IV. Besides, one can see that the E_b/I_0 performance of the two omnidirectional cases are very close. This is because in Schemes I and II most interfering signals during downlink transmissions are from base stations and their interference scenarios are similar.

Fig. 15 shows the call blocking performance of the four different allocation schemes. We can see that the proposed Scheme III has the same call blocking performance as the omnidirectional antenna case, i.e., Scheme II. Recall that Scheme III ag-

gregates all the codes/time slots of the three sectors in a virtual cell and then assigns these time slot/codes to the covered mobile terminals, while Scheme II assigns codes/time slots to mobile terminals in a cell with omnidirectional antenna. Since a virtual cell has the same coverage area and the same number of codes/time slots as an omnicell, the call blocking probability of the two schemes perform closely. However, Scheme II has poor radio link performance as shown in Figs. 13 and 14. In Scheme I, an optimal switching point setting is required for the global uplink/downlink bandwidth ratio among all the cells within the entire system. If adopting a global uplink/downlink bandwidth ratio as in Scheme I, each cell may sacrifice its actual traffic requirement, thereby causing higher call blocking than Schemes II and III. The blocking rate of Scheme IV is very high due to the decrease of trunking efficiency. Observing from Figs. 13, 14, and 15, we can conclude that the proposed virtual cell-based resource allocation in TDD-CDMA systems with trisector cellular architecture can have the best E_b/I_0 performance, while maintaining good blocking rate performance.

VII. Conclusion

In this paper, we have developed an analytic framework to evaluate the interference of the TDD-CDMA system with directional antennas and asymmetric services. Our results show that the strong cross-slot interference in the TDD-CDMA system will be restricted into a small area, namely a virtual cell, if a trisector directional antennas are employed at base stations. It is found that the directivity of sector antennas can provide additional degree of freedom for allocating radio resources, which inspires us to design a virtual cell-based code/time slot assignment scheme to allocate radio resource in the TDD-CDMA system. Through simulation, we have demonstrated that by coordinating the switching point setting of only three sectors in a virtual cell, the proposed simple code/time slot allocation algorithm can substantially reduce the strong base-to-base and mobile-to-mobile cross-slot interference, while maintaining good call blocking performance. Therefore, through the virtual cell-based code/time slot assignment algorithm in the trisector cellular structure, the TDD-CDMA system can have a greater flexibility in supporting asymmetric service by allowing independently setting on the rates of asymmetry in every small area within the entire system.

Some interesting future research topics that can be extended from this work includes the issue of designing an optimal dynamic switching point setting algorithm in the context of virtual cell based TDD/CDMA system. Furthermore, in a TDD/CDMA system employed with the more advanced beamforming antenna technique, developing an efficient resource allocation algorithm is still an important issue. In [4], it is found that although beamforming antennas can effectively alleviate the base-to-base cross-slot interference, the mobile-to-mobile cross-slot interference can still be a problem because a mobile terminal cannot be easily equipped with multiple antennas. Accordingly, for a TDD-CDMA system equipped with beamforming antennas at base stations, how to develop an efficient resource allocation algorithm becomes inevitable from the aspect of overcoming the mobile-to-mobile cross-slot interference.

References

[1] M. Haardt, A. Kleig, R. Koehn, M. Purat, V. Sommer, and T. Ulrich, "The TD-CDMA based TRRA TDD mode," *IEEE J. Sel. Areas Commun.*, vol. 18, no. 8, pp. 1375–1385, Aug. 2000.

[2] X. Wu, L.-L. Yang, and L. Hanzo, "Uplink capacity investigations of TDD-CDMA," in *IEEE Veh. Technol. Conf.*, Spring 2002, pp. 997–1001.

[3] H. Holma, G. J. R. Povey, and A. Toskala, "Evaluation of interference between uplink and downlink in UTRA/TDD," in *IEEE Veh. Technol. Conf.*, Fall 1999, pp. 2616–2620.

[4] C.-J. Chen and L.-C. Wang, "Suppressing opposite direction interference in TDD systems with asymmetric traffic using antenna beam-forming," *IEEE Trans. Veh. Technol.*, vol. 53, no. 4, pp. 956–967, Jul. 2004.

[5] D. G. Jeong and W. S. Jeon, "Time slot allocation in CDMA/TDD systems for mobile multimedia services," *IEEE Commun. Lett.*, vol. 4, no. 2, pp. 59–61, Feb. 2000.

[6] W. S. Jeon and D. G. Jeong, "Comparison of time slot allocation strategies for CDMA/TDD systems," *IEEE J. Sel. Areas Commun.*, vol. 18, no. 7, pp. 1271–1278, Jul. 2000.

[7] H. Haas, S. McLaughlin, and G. J. R. Povey, "A novel interference resolving algorithm for the TDD TD-CDMA mode in UMTS," *IEEE Pers., Indoor and Mobile Radio Commun.*, pp. 1231–1235, 2000.

[8] O. Lehtinen and J. Kurjenniemi, "UTRA TDD dynamic channel allocation in uplink with slow reallocation," in *IEEE Veh. Technol. Conf.*, Spring 2003, pp. 1401–1405.

[9] H. Holma, S. Heikkinen, O.-A. Lehtinen, and A. Toskala, "Interference considerations for the time division duplex mode of the UMTS terrestrial radio access," *IEEE J. Sel. Areas Commun.*, vol. 18, no. 8, pp. 1386–1393, Aug. 2000.

[10] L.-C. Wang, S.-Y. Huang, and Y.-C. Tseng, "A novel interference-resolving algorithm to support asymmetric services in TDD-CDMA systems with directional antennas," in *IEEE Veh. Technol. Conf. (VTC'02 Spring)*, May 2002, pp. 327–330.

[11] S. S. Choi and D. H. Cho, "Coordinated resource allocation scheme for forward link in sectorized CDMA systems," in *IEEE Veh. Technol. Conf. (VTC'02 Fall)*, Sep. 2002, pp. 2356–2360.

[12] K. Pahlavan and A. Levesque, *Wireless Information Networks*. New York: Wiley, 1995.

[13] K. S. Gilhousen, I. M. Jacob, R. Padovani, A. J. Viterbi, L. A. Weaver, and C. E. Wheatley, "On the capacity of a cellular CDMA system," *IEEE Trans. Veh. Technol.*, vol. 40, no. 2, pp. 303–3128, May 1991.

[14] J.-P. Linnartz, *Narrowband Land-Mobile Radio Networks*. Norwood, MA, 1993, pp. 325–326.

Li-Chun Wang (S'92–M'96) received the B.S. degree from National Chiao Tung University, Hsinchu, Taiwan, in 1986, the M.S. degree from National Taiwan University in 1988, and the Ms.Sci. and Ph.D. degrees in electrical engineering from the Georgia Institute of Technology, Atlanta, in 1995, and 1996, respectively.

From 1990 to 1992, he was with the Telecommunications Laboratories of the Ministry of Transportations and Communications in Taiwan (currently the Telecom Labs. of Chunghwa Telecom Co.). In 1995, he was with Bell Northern Research of Northern Telecom, Inc., Richardson, TX. From 1996 to 2000, he was with AT&T Laboratories, where he was a Senior Technical Staff Member in the Wireless Communications Research Department. Since August 2000, he has been an Associate Professor with the Department of Communication Engineering of National Chiao Tung University. His current research interests are in the areas of cellular architectures, radio network resource management, and cross-layer optimization for high speed wireless networks. He holds three U.S. patents and one more pending.

Dr. Wang was a corecipient of the Jack Neubauer Memorial Award in 1997 recognizing the Best Systems Paper published in the IEEE Transactions on Vehicular Technology. Currently, he is the Editor of the IEEE Transactions on Wireless Communications.

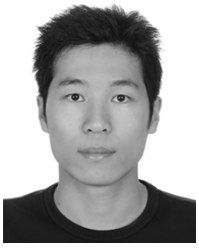

Shi-Yen Huang received the B.S. and M.S. degrees in communication engineering from the National Chiao Tung University, Hsinchu, Taiwan, in 2001 and 2003, respectively.

He is currently working on his national service and planning to study for the Ph.D. degree in the future. His research interests include the wireless communication system and network performance analysis.

Yu-Chee Tseng received the B.S. and M.S. degrees in computer science from the National Taiwan University and the National Tsing-Hua University, Taiwan, in 1985 and 1987, respectively. He received the Ph.D. degree in computer and information science from the Ohio State University, Columbus, in 1994.

In 1990, he was an engineer with D-LINK Inc. From 1994–1996 , he was an Associate Professor with Chung-Hua University and with National Central University (1996–1999), and a Full Professor with National Central University during 1999–2000. Since 2000, he has been a Full Professor with the Department of Computer Science and Information Engineering, National Chiao-Tung University, Hsinchu, Taiwan. His research interests include mobile computing, wireless communication, network security, and parallel and distributed computing.

Dr. Tseng served as a Program Chair of the Wireless Networks and Mobile Computing Workshop, 2000 and 2001, as a Vice Program Chair of the International Conference on Distributed Computing Systems (ICDCS), 2004, and as a Vice Program Chair of the IEEE International Conference on Mobile Ad-hoc and Sensor Systems (MASS), 2004. He served as an Associate Editor for *The Computer Journal*, as a Guest Editor for the *ACM Wireless Networks* Special ISsue on "Advances in Mobile and Wireless Systems." He served as Guest Editor for the IEEE TRANSACTIONS ON COMPUTERS Special Issue on "Wireless Internet," as a Guest Editor for the *Journal of Internet Technology* Special Issue on "Wireless Internet: Applications and Systems," as a Guest Editor for *Wireless Communications and Mobile Computing* Special Issue on "Research in Ad Hoc Networking, Smart Sensing, and Pervasive Computing," as an Editor for the *Journal of Information Science and Engineering*, as a Guest Editor for *Telecommunication Systems* Special Issue on "Wireless Sensor Networks," and as a Guest Editor for the *Journal of Information Science and Engineering* Special Issue on "Mobile Computing." He is a two-time recipient of the Outstanding Research Award, National Science Council, ROC, in 2001–2002 and 2003–2005, and a recipient of the Best Paper Award in International Conference on Parallel Processing, 2003. Several of his papers have been chosen as Selected/Distinguished Papers in international conferences. He has guided students to participate in several national programming contests and received several awards. Dr. Tseng is a member of ACM.